Temporal changes in mouse aortic wall gene expression during the development of elastase-induced abdominal aortic aneurysms

Sarah J. Van Vickle-Chavez, BA,[a] William S. Tung, MD,[a] Tarek S. Absi, MD,[a] Terri L. Ennis, BS,[a] Dongli Mao, MD,[a] J. Perren Cobb, MD,[a] and **Robert W. Thompson, MD,[a,b,c]** *St Louis, Mo*

Objective: **To characterize temporal changes in mouse aortic wall gene expression associated with the development of experimental abdominal aortic aneurysms.**

Methods: **C57BL/6 mice underwent transient perfusion of the abdominal aorta with either elastase (n = 61) or heat-inactivated elastase as a control (n = 68). Triplicate samples of radiolabeled aortic wall complementary DNA were prepared at intervals of 0, 3, 7, 10, and 14 days, followed by hybridization to nylon microarrays (1181 genes). Autoradiographic intensity data were normalized by conversion to *z* scores, and differences in gene expression were defined by two-tailed *z* tests at a significance threshold of $P < .01$.**

Results: **Elastase perfusion caused a progressive increase in aortic diameter up to 14 days accompanied by transmural inflammation and destructive remodeling of the elastic media. No aneurysms occurred in the control group. Compared with healthy aorta, 336 genes exhibited significant alterations during at least 1 interval after elastase perfusion (135 at more than 1 interval and 14 at all intervals), with pronounced increases for interleukin 6, cyclin E2, interleukin 1β, osteopontin, CD14/lipopolysaccharide receptor, P-selectin glycoprotein ligand 1, and gelatinase B/matrix metalloproteinase 9 (all >20-fold on day 3). Sixty-two genes exhibited synchronous alterations in the elastase and control groups, thus suggesting a nonspecific response. By direct comparisons between the elastase and control groups, there were 384 genes with significant differences in expression for at least 1 interval after aortic perfusion, including 234 with differential upregulation (eg, p44MAPK/ERK1, osteopontin, heat shock protein 84, hypoxia-inducible factor 1α, apolipoprotein E, monocyte chemotactic protein 3, MIG (monokine induced by gamma interferon), and interleukin 2 receptor γ) and 163 with differential downregulation (eg, prothrombin, granzyme B, ataxia telangiectasia mutated, and interleukin-converting enzyme).**

Conclusions: **Development of elastase-induced abdominal aortic aneurysms in mice is accompanied by altered aortic wall expression of genes associated with acute and chronic inflammation, matrix degradation, and vascular tissue remodeling. Knowledge of these alterations will facilitate further studies on the functional molecular mechanisms that underlie aneurysmal degeneration. (J Vasc Surg 2006;43:1010-20.)**

Understanding the cellular and molecular mechanisms that underlie the development of abdominal aortic aneurysms (AAAs) remains an active area of interest. To better elucidate the molecular changes that occur in AAAs, complementary DNA (cDNA) microarrays have been used to profile differences in gene expression between normal human aorta and aneurysm tissues.[1-3] Although this approach provides insight into the genes expressed in end-stage human AAA tissues, it is unclear how these alterations relate to the dynamic processes involved in earlier or progressive stages of disease. An alternative approach to address this question is by examining aortic wall gene expression in experimental animal models of AAAs, which have already provided a useful means of investigating the pathophysiologic mechanisms that underlie aneurysmal degeneration.[4,5]

Transient aortic perfusion with pancreatic elastase is one of the most widely used experimental models of AAAs.[4,5] Although elastase perfusion does not immediately result in aneurysm formation, it initiates a process of aortic wall infiltration by mononuclear phagocytes, increased local expression of endogenous proteinases, progressive elastin degradation, and gradual aortic wall dilation.[6,7] Because

From the Departments of Surgery,[a] Radiology,[b] and Cell Biology and Physiology,[c] Washington University School of Medicine.

Supported by grants R01 HL64332 and R01 HL64333 from the National Heart, Lung, and Blood Institute (RWT) and by an award for Excellence in Vascular Surgical Research for Residents, Fellows, and Mentors from the William J. von Liebig Foundation. JPC was supported by the George H. A. Clowes, Jr, Memorial Research Career Development Award from the American College of Surgeons and by grant R01 GM059960 from the National Institute for General Medical Sciences.

Competition of interest: Dr Thompson has previously received research project grant support from Medtronic, Inc (Santa Rosa, Calif) and from Cordis/Johnson & Johnson for research projects unrelated to this article.

Presented at the Second American Heart Association Conference on Arteriosclerosis, Thrombosis, and Vascular Biology, Arlington, Va, May 11-13, 2001.

Reprint requests: Robert W. Thompson, MD, Section of Vascular Surgery, Washington University School of Medicine, 9901 Wohl Hospital, 4960 Children's Place, St Louis, MO 63110 (e-mail: thompsonr@msnotes.wustl.edu).

0741-5214/$32.00

doi:10.1016/j.jvs.2006.01.004

these lesions follow a highly predictable time course accompanied by histopathologic changes that mirror those found in human AAAs, elastase-induced AAAs have been used to demonstrate the functional importance of proinflammatory cytokines, prostaglandins, and matrix metalloproteinases (MMPs) in aneurysm disease, as well as effective suppression of AAAs by using various anti-inflammatory agents and proteinase inhibitors.[8-11] Adaptation of this model to genetically altered mice has also made it possible to delineate the functional importance of specific gene products in the process of aneurysm formation.[12-15]

Given the potential insights into disease mechanisms that might be obtained through more comprehensive understanding of the elastase-induced mouse model of AAAs, we sought, by use of cDNA microarray techniques, to systematically characterize the temporal alterations in aortic wall gene expression that accompany aneurysm development. Our results confirm that experimental AAAs involve altered patterns of expression for many genes associated with acute and chronic inflammation, matrix degradation, and vascular tissue remodeling, as well as several matricellular glycoproteins not previously associated with aneurysm disease. This systematic approach has thereby helped to identify regulatory pathways and putative therapeutic targets in aneurysmal degeneration, thus providing an important basis for further investigation.

METHODS

A complete description of all methods is provided online.

Elastase perfusion model. All experimental procedures were performed in accord with a protocol approved by the Animal Studies Committee at Washington University School of Medicine. Adult male C57BL/6J mice (Jackson Laboratory, Bar Harbor, Me) were subjected to transient intraluminal perfusion of the infrarenal aorta with either elastase (n = 61) or heat-inactivated elastase for controls (n = 68), as previously described.[12,16]

Radiolabeled cDNA probes and membrane hybridization. Animals were killed on days 3, 7, 10, and 14 after perfusion with elastase or heat-inactivated elastase, along with additional mice to provide normal aortic tissues. Aortic tissues were snap-frozen at −70 °C and divided into three equal subgroups for each experimental condition, and the tissues for each subgroup were pooled as triplicate samples (each pool contained up to eight aortic specimens). All subsequent steps were thereafter performed by using triplicate samples for each experimental condition for a total of 27 separate microarrays. Pooled aortic tissue samples were pulverized under liquid nitrogen, total RNA was isolated, and ^{33}P-labeled cDNA probes were prepared with reagents and protocols provided with the Atlas Mouse 1.2 cDNA Expression Array kit from Clontech Laboratories, Inc (Palo Alto, Calif). Each labeled cDNA probe sample was incubated with a nylon membrane containing cDNA clones corresponding to 1181 known murine genes (AtlasArray Mouse 1.2; Clontech). After autoradiography, densitometry readings for each gene were adjusted for background readings on the same membrane.

Data analysis and estimates of statistical significance. Densitometry signal intensities were transformed to *z* scores to normalize the data from each microarray.[17] The average *z* score was determined for each gene at each time interval for each of the experimental groups. The significance of differences in gene expression was evaluated by using the two-sample-for-means *z* test to maximize the power of replicates and to take into account variation between replicates on a gene-by-gene basis.[17] *P* values were assigned to the calculated *z* test values, and the threshold for statistical significance was set at $P < .01$ for all comparisons between groups. The n-fold changes in gene expression were calculated, and temporal changes in gene expression were plotted for selected genes by using the mean ± SE of converted *z*-score values.

RESULTS

Time course of aneurysm development. There was a moderate increase in mouse aortic diameter (AD) (approximately 50%) immediately after perfusion with either elastase or heat-inactivated elastase, but in no case did this reach aneurysmal proportions (Fig 1, *A* and Table A, online only). In the elastase-perfused group, there was a gradual increase in AD between days 3 and 10, followed by more rapid dilatation between days 10 and 14. In contrast, AD remained stable throughout the 14-day experimental period in the control group, without either gradual dilatation or rapid secondary expansion. Light microscopy revealed minimal disruption of the elastic media immediately and up to 3 days after aortic perfusion in both the elastase-perfused and control groups, and each group exhibited early infiltration of inflammatory cells into the outer aortic wall (Fig 1, *B*). In the elastase-perfused group, these initial structural changes were followed at later time intervals by progressive transmural aortic wall infiltration by mononuclear phagocytes and destruction of the elastic lamellae; in contrast, the acute inflammatory response in the control group was resolved by day 7, and the elastic lamellae were structurally intact at later intervals. The temporal progression of aneurysm development and the sequence of histologic changes observed were therefore consistent with previous studies using the elastase-induced mouse model of AAAs. This emphasizes the close associations among the delayed onset of chronic aortic wall inflammation, progressive degradation of medial elastin, and aneurysmal dilation.[12,16] These findings also demonstrate that the time intervals selected for gene expression analysis were pathophysiologically relevant in the stepwise progression of experimental AAAs.

Alterations in aortic wall gene expression at various intervals after elastase perfusion compared with normal aorta. In the initial data analysis, differences in aortic wall gene expression were examined between normal aorta and the tissues obtained at each interval from the elastase-perfused and control groups. There were 336 of 1181 genes expressed at significantly altered levels for at least 1 time interval after elastase perfusion, 135 were altered at more than 1 interval, and 14 were altered at all 4 intervals (Table B, online only). Table I indicates the genes with the

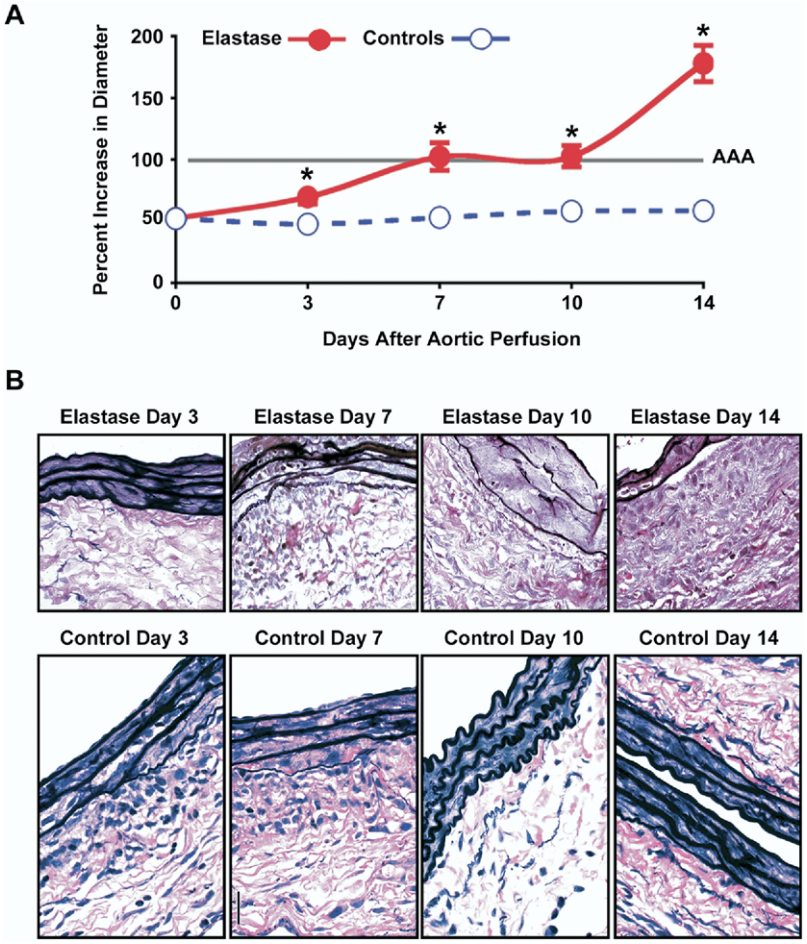

Fig 1. Aortic dilatation and structural changes during the development of elastase-induced abdominal aortic aneurysms *(AAAs)*. **A,** Percentage of aortic dilatation at various intervals after perfusion with elastase or heat-inactivated elastase (controls). Data shown reflect the mean ± SE. The threshold for definition of AAAs is indicated by the horizontal line. **P* < .001, elastase vs controls, Mann-Whitney test. **B,** Representative sections of mouse aortic tissue obtained at various intervals after perfusion with elastase or heat-inactivated elastase (controls) (stain, Verhoeff–van Gieson; original magnification, ×40).

most pronounced increases or decreases after elastase perfusion (all >20-fold or <50-fold compared with normal aorta); the temporal patterns of expression for selected genes are shown in Figs 2 and 3. A complete list of these genes is provided in Table C (online only).

Alterations in the heat-inactivated elastase control group compared with normal aorta. Comparisons between normal aortas and the control group revealed that 376 of 1181 genes were expressed at significantly different levels for at least 1 time interval after perfusion with heat-inactivated elastase, 146 were altered at more than 1 interval, and 10 were altered at all 4 intervals (Tables B and D, online only). This included 62 genes with synchronous changes in aortic wall expression in both the elastase and control groups compared with normal aorta, thus indicating that they represent common patterns of response to injury rather than alterations unique to elastase-induced aneurysm development (Tables B and E, online only).

Differential gene expression between the elastase and control groups. In the second stage of data analysis, temporal differences in gene expression unique to the development of elastase-induced AAAs were examined by directly comparing data between animals undergoing perfusion with elastase vs heat-inactivated elastase controls at each time interval. Significantly different levels of expression were detected for 384 of 1181 genes during at least 1 time interval after aortic perfusion, with 85 at more than 1 interval and 17 at 3 intervals (Table B, online only). Transcripts with the most pronounced differential increases (>20-fold) and decreases (>-50-fold) are shown in Tables II and Table III, respectively, and the complete list of genes with differential expression is shown in Table F (online only).

It is noteworthy that this analysis revealed prominent differential expression for many genes in the following functional categories:

Table I. Genes with pronounced alterations in aortic wall expression at various intervals following perfusion elastase vs normal aorta (partial list)

Increased > 20-Fold vs Normal		*Decreased > 50-Fold vs Normal*	
Elastase Day 3	*Fold*	*Elastase Day 3*	*Fold*
interleukin-6 (16193)	61	norepinephrine transporter (20538)	−53
G1/S-specific cyclin E2 (12448)	473	K channel (16497)	−53
interleukin-1 beta (16176)	291	insulin receptor substrate-1 (16367)	−56
osteopontin (20750)	211	5-HT receptor-2 (15558)	−57
ephrin receptor B2 (13844)	192	oxytocin receptor (18430)	−57
CD14/LPS receptor (12475)	59	caspase-11 (12363)	−59
integrin beta-2/CD18 (16414)	37	granzyme B (14939)	−61
P-selectin GP ligand 1 (20345)	30	glutamate receptor delta 1 (14803)	−61
frizzled-related sequence 3 (20378)	30	CRF receptor (12921)	−61
semaphorin J (20354)	211	stromelysin-3/MMP-11 (17385)	−65
gelatinase B (17395)	29	caspase-7 (12369)	−71
paired box protein-2/PAX2 (18504)	26	neuronal death protein 5 (12123)	−77
serine protease inhibitor 2-2 (20716)	26	calcium-binding ALG2 (18570)	−78
basic HLH mesoderm post 2 (17293)	24	K voltage gated channel (16500)	−80
anterior-restricted homeobox (15209)	22	interleukin-converting enzyme (12362)	−85
CDK interacting CIP1/WAF1 (12575)	22	protease inhibitor-17 (20713)	−141
SOCS-3 (12702)	21	*Elastase Day 7*	*Fold*
Elastase Day 7	*Fold*	alpha-1-antitrypsin 1-2 (20701)	−51
interleukin-1 beta (16176)	259	caspase-11 (12363)	−65
osteopontin (20750)	161	RalGDSB (19730)	−80
brachiury T-box gene (20997)	47	guanylate cyclase soluble beta-1 (54195)	−81
octamer-binding 6 (18991)	33	tubulin beta 4 (22153)	−84
P-selectin GP ligand 1 (20345)	32	interleukin-converting enzyme (12362)	−93
semaphorin J (20354)	32	connexin 45 (14615)	−150
NIMA-related (18005)	30	*Elastase Day 10*	*Fold*
c-fgr proto-oncogene (14191)	26	MAPKK4/JNKK1 (26398)	−50
tolloid-like protein (21892)	26	zinc finger protein GLI3 (14634)	−51
interferon beta (15977)	25	pou domain class 6F1 (19009)	−58
del. in colorectal carcinoma (13176)	25	ephrin receptor A7 (13841)	−61
bub1B mitotic checkpoint (12236)	23	eyes absent homolog 1 (EYA1) (14048)	−63
Elastase Day 10	*Fold*	hemat. expr. homeobox HHEX (15242)	−64
G1/S-specific cyclin E2 (12448)	784	semaphorin E (20348)	−112
glutamate receptor epsilon 1 (14811)	329	integrin alpha 7 (16404)	−155
osteopontin (20750)	30	*Elastase Day 14*	*Fold*
prepro-orexin (15171)	166	neurogenin 3 (11925)	−56
serine protease inhibitor 2-2 (20716)	63	GABA-A receptor alpha-1 (14394)	−59
frizzled-related sequence 3 (20378)	34	homeobox protein D12 (15432)	−59
integrin beta-2/CD18 (16414)	31	single-minded homolog 1 (20464)	−66
myb-related protein B (17865)	28	homeobox protein GSH2 (14843)	−72
Rab-3b (69908)	27	purinergic receptor P2Y (18441)	−75
IGF-binding protein 1 (16006)	24	integrin alpha 3 (16400)	−80
del. in colorectal carcinoma (13176)	23	VIP receptor 2 (22355)	−85
Elastase Day 14	*Fold*	oxytocin receptor (18430)	−109
interleukin-1 beta (16176)	201	cone-rod homeobox (12951)	−110
YY1 transcription factor (22632)	185	5-HT receptor 1B (15551)	−375
osteopontin (20750)	112		
serine protease inhibitor 2-2 (20716)	49		
P-selectin GP ligand 1 (20345)	35		
semaphorin J (20354)	34		
ShcC adaptor (20418)	30		
CD14/LPS receptor (12475)	30		

Analysis of the expression profiling dataset was used to initially identify significant alterations in aortic wall gene expression at various intervals after elastase perfusion compared to normal aorta. The significance threshold for data analysis was set at $P < 0.01$ using the 2-tailed Z test, and genes were listed in rank-order based on the calculated relative fold-changes. Genes shown here include those with increased expression of at least 20-fold or decreased expression of at least −50-fold compared to normal aorta, excluding genes with synchronous alterations in the elastase and heat-inactivated elastase control groups (the complete list of genes with distinct alterations in expression following elastase perfusion is shown in **Supplementary Data Table C**, on-line only). Gene ID numbers (shown in parentheses) refer to the Entrez Gene database at the National Center for Biotechnology Information (NCBI; http://www.ncbi.nlm.nih.gov/entrez/query.fcgi?db=gene).

1. Cytokines and chemokines—increases for interleukin (IL)-1β (Fig 2, *B*), monocyte chemotactic protein (MCP)-3 (Fig 2, *C*), MIG (Fig 2, *G*), and suppressor of cytokine signaling 1.
2. Proteinases and protease inhibitors—increases for urokinase and granzyme C and decreases for anti-leukoproteinase 1, protease inhibitor 17, prothrombin, granzyme B, antithrombin III, plasminogen, α_1-

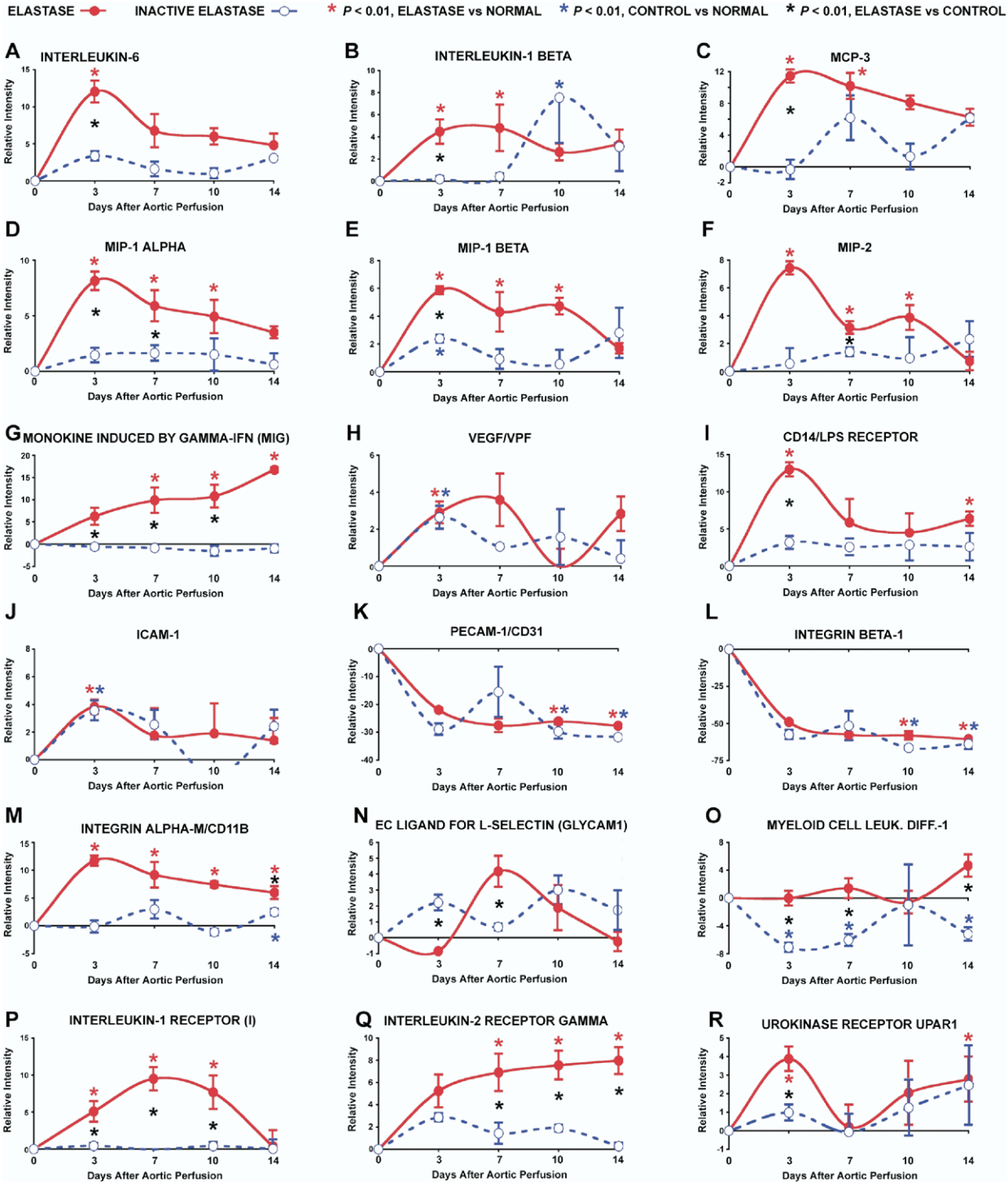

Fig 2. Temporal expression profiles for selected cytokines, chemokines, adhesion molecules, and cellular receptors. Relative patterns of expression after aortic perfusion with elastase vs heat-inactivated elastase controls are shown for selected genes. **(A)** Interleukin 6 (gene ID 16193), **(B)** interleukin 1β (gene ID 16176), **(C)** monocyte chemotactic protein *(MCP)*-3 (gene ID 20306), **(D)** MIP-1α (gene ID 20302), **(E)** MIP-1β (gene ID 20303), **(F)** MIP-2 (gene ID 20310), **(G)** MIG (gene ID 17329), **(H)** vascular endothelial growth factor *(VEGF)*/vascular permeability factor *(VPF)* (gene ID 22339), **(I)** CD14/lipopolysaccharide *(LPS)* receptor (gene ID 12475), **(J)** ICAM-1 (gene ID 15894), **(K)** platelet endothelial cell adhesion molecule *(PECAM)*-1/CD31 (gene ID 18613), **(L)** integrin β1 (gene ID 16412), **(M)** integrin αM (gene ID 16409), **(N)** endothelial ligand for L-selectin (glycam 1; gene ID 14663), **(O)** myeloid cell leukemia differentiation antigen (gene ID 17210), **(P)** interleukin 1 receptor (gene ID 16177), **(Q)** interleukin 2 receptor γ (gene ID 16186), and **(R)** urokinase receptor (*uPAR*; gene ID 18793).

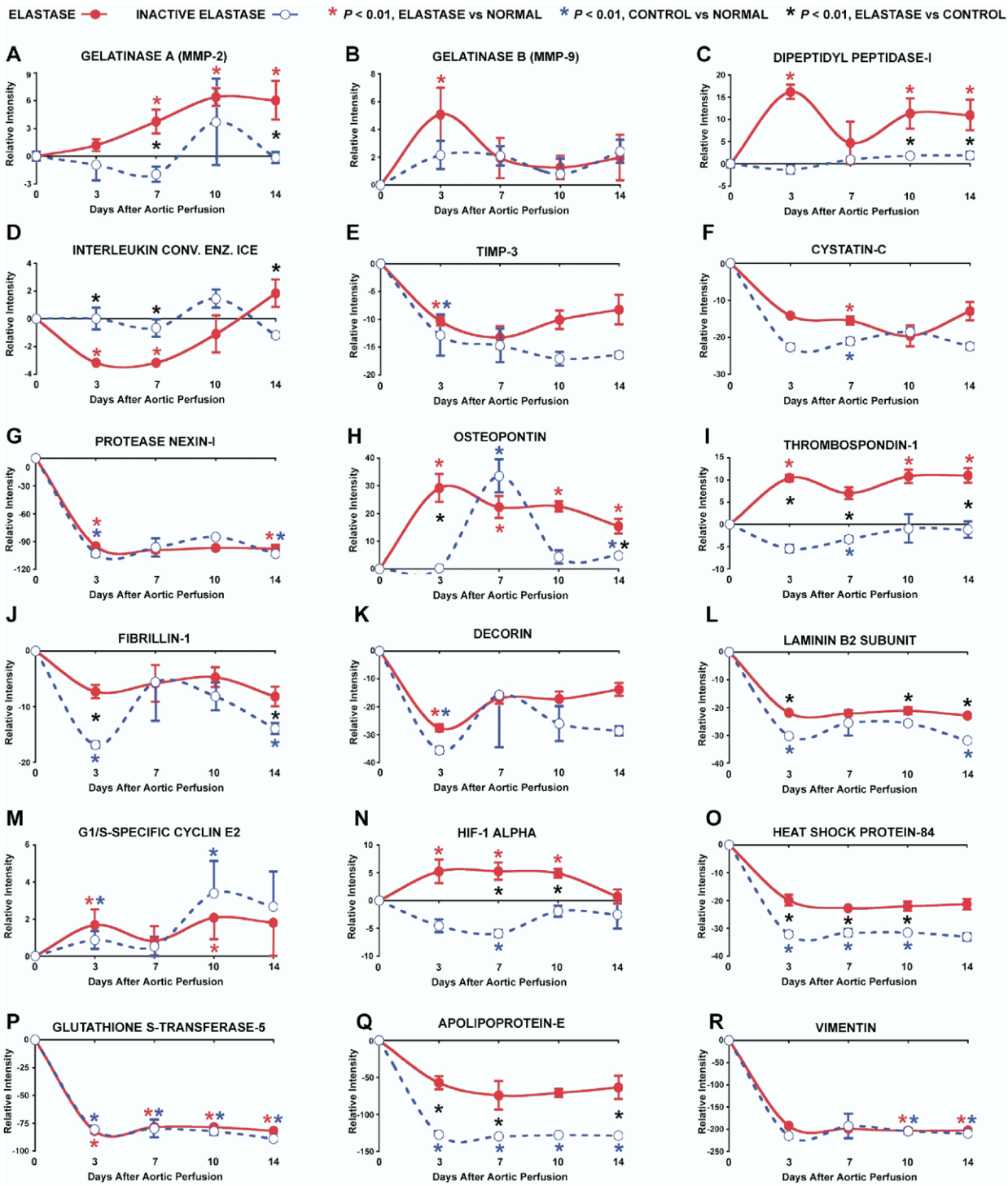

Fig 3. Temporal expression profiles for selected proteinases, protease inhibitors, extracellular matrix proteins, and proteins involved in cellular metabolism, stress response, and growth/apoptosis. Relative patterns of expression after aortic perfusion with elastase vs heat-inactivated elastase controls are shown for selected genes. **(A)** Gelatinase A/matrix metalloproteinase *(MMP)*-2 (gene ID 17390), **(B)** gelatinase B/MMP-9 (gene ID 17395), **(C)** dipeptidyl peptidase I (cathepsin C; gene ID 13032), **(D)** interleukin-converting enzyme (*ICE*; gene ID 12362), **(E)** TIMP-3 (gene ID 21859), **(F)** cystatin C (gene ID 13010), **(G)** protease nexin I (gene ID 20720), **(H)** osteopontin (gene ID 20750), **(I)** thrombospondin 1 (gene ID 21825), **(J)** fibrillin 1 (gene ID 14118), **(K)** decorin (gene ID 13179), **(L)** laminin B2 (gene ID 226519), **(M)** cyclin E2 (gene ID 12448), **(N)** hypoxia-inducible factor *(HIF)*-1α (gene ID 15251), **(O)** heat shock protein 84 (gene ID 15516), **(P)** glutathione-*S*-transferase 5 (GST-5; gene ID 14863), **(Q)** apolipoprotein E (gene ID 11816), and **(R)** vimentin (gene ID 22352).

Table II. Genes with the largest differential increases (> 20-fold) in aortic wall expression at various intervals following perfusion with elastase vs heat-inactivated elastase controls

Day 3 After Aortic Perfusion	*Fold*
p44-MAPK/ERK1 (26417)	589
osteopontin (20750)	575
abl proto-oncogene (11350)	550
c-myc proto-oncogene (17869)	525
BAX protein alpha (12028)	380
cdk-inhibitor kip2 (12577)	275
ephrin receptor A7 (13841)	269
ezrin (22350)	269
myo. dyst. assoc. DMAHP (20475)	263
fibrillin 1 (14118)	200
wingless-related WNT6 (22420)	200
MCP-3 (20306)	195
fos-related antigen-2/FRA2 (14284)	138
Rb binding protein-6 (19647)	102
SMAD3 (17127)	87
distal-less homeobox-6 (13396)	87
interleukin-1 beta (16176)	83
SOCS-1 (12703)	83
adenosine A3 receptor (11542)	78
DNA ligase I (16881)	76
fibroblast growth factor-9 (14180)	74
urokinase/uPA (18792)	74
activin type IIA receptor (11480)	72
cytokeratin-19 (16669)	69
heat shock transc. factor 2 (15500)	66
monocarboxylate transporter (20501)	63
adenosine A2A receptor (11540)	58
Ca-activated K channel beta (16533)	56
Rab GDI alpha (14567)	54
LIM domain kinase 1 (16885)	50
ick proto-oncogene (16818)	49
cdc25MM (19417)	36
apolipoprotein E (11816)	24
Day 7 After Aortic Perfusion	*Fold*
calpactin I light chain (20194)	335
osteoblast-specific OSF2 (50706)	316
HIF-1 alpha (15251)	275
apolipoprotein E (11816)	275
btb & cnc homolog 1 (12013)	263
Day 7 After Aortic Perfusion (Cont)	*Fold*
NIMA-related protein kinase-2 (18005)	182
huntingtin-associated protein 1 (15114)	138
glucocorticoid receptor 1 (14815)	117
cytokeratin 14 (16664)	102
Day 10 After Aortic Perfusion	*Fold*
clusterin/apolipoprotein J (12759)	355
purine-rich binding A/PURA (19290)	295
int-3 proto-oncogene/notch4 (18132)	219
MAPKK3/MEK3 (26406)	162
acetylcholine receptor delta (11447)	135
gIFN-induced monokine MIG (17329)	117
homeobox protein 3.1 (15426)	93
secreted apoptosis-related prot. 1 (20319)	79
interferon regulatory factor 1 (16362)	72
p18 ckd inhibitor INK6 (12580)	51
follistatin (14313)	48
zinc finger protein 144 (22658)	44
Ca-activated K channel beta (16533)	44
protein kinase C theta (18761)	42
Marcks-related protein (17357)	23
Day 14 After Aortic Perfusion	*Fold*
gut Kruppel-like factor (16600)	513
granzyme C (14940)	437
nucleoside diphosphate kinase B (18103)	437
transferrin receptor (22042)	398
mdm2 (17246)	347
zinc transporter-4 (22785)	282
caspase-activated DNase (13368)	240
huntingtin-associated protein 1 (15114)	174
special AT-rich binding 1 (20230)	138
apolipoprotein E (11816)	91
formin-4 (14260)	76
semaphorin E (20348)	74
prepro-endothelin-3 (13616)	68
BAD protein (12015)	66
STRA13 (16792)	65
phenylalanine-4-hydroxylase (18478)	50
guanine nucl. binding alpha, stim. (14683)	32
disabled homolog 2 (13132)	22

Analysis of the expression profiling dataset was used to identify significant differences in aortic wall gene expression at various intervals between the elastase perfusion groups compared to controls. The significance threshold for data analysis was set at $P < 0.01$ using the 2-tailed Z test, and genes were listed in rank-order based on the calculated relative fold-changes. Genes shown here include those with increased expression of at least 20-fold in the elastase group compared to the heat-inactivated elastase control group (the complete list of genes with differential expression following elastase perfusion is shown in **Supplementary Data Table F**, on-line only).

antitrypsin 1 and 2, and IL-converting enzyme (Fig 3, *D*).

3. Adhesion proteins and receptors—decreases for cadherin 8, cadherin 15, estrogen-related receptor α, integrin α_2, and endothelial ligand for L-selectin (Fig 2, *N*).
4. Extracellular matrix proteins—increases for osteopontin (Fig 3, *H*) and fibrillin 1 (Fig 3, *J*) and decreases for collagen 9α1.
5. Proteins involved in immune response—decreases for T-cell activation antigen CD27, V(D)J recombination activating protein RAG-1, and T-cell linker ZAP-70.
6. Proteins involved in metabolism, oxidative stress, and cell growth/apoptosis—increases for the *abl* proto-oncogene, c-*myc* proto-oncogene, fibroblast growth factor 9, caspase-activated deoxyribonuclease, BAXα, BAD, apolipoprotein E (Fig 3, Q), and hypoxia-inducible factor 1α (Fig 3, N) and decreases for ataxia telangiectasia mutated and caspase 11.

DISCUSSION

In this study, we applied cDNA expression profiling to an inducible mouse model of experimental AAAs to better understand the molecular changes that occur during aneurysm development. Our study is therefore similar in design to that recently reported by Yajima et al,[18] in which cDNA microarrays were used to examine aortic wall gene expression in the elastase-induced rat model of AAAs. The most significant findings of this study are as follows: (1) experimental AAAs are associated with an early increase in expression of genes involved in the acute-phase innate immune response, leukocyte recruitment, and the transition to chronic inflammation; (2)

Table III. Genes with the largest differential decreases (> −50-fold) in aortic wall expression at various intervals following perfusion with elastase vs heat-inactivated elastase controls

Day 3 After Aortic Perfusion	*Fold*
androgen receptor (11835)	−50
gem induced immed. early (14579)	−50
oxytocin receptor (18430)	−55
neural CAM-2 (17968)	−58
ack tyrosine-protein kinase (51789)	−60
antileukoproteinase-1 (20568)	−66
K voltage gated channel (16500)	−66
caspase-11 (12363)	−69
T-cell activation CD27 (21940)	−69
tryptophan 5-hydroxylase (21990)	−71
interleukin-6 receptor alpha (16194)	−71
NIMA-rel. protein kinase 3 (23954)	−76
V(D)J recomb. activ. RAG-1 (19373)	−79
collagen 9 alpha-2/COL9A2 (12840)	−81
src-related intestinal kinase (20459)	−83
alpha 2 catenin (12386)	−83
galanin receptor 1 (14427)	−87
unconventional myosin VI (17920)	−87
glutamate receptor alpha 1 (14799)	−87
BMP receptor type 1B (12167)	−89
mem. metalloendopeptidase (17380)	−89
T-cell transcription GATA3 (14462)	−91
protease inhibitor-17 (20713)	−93
interleukin-converting ICE (12362)	−93
zinc transporter-4 (22785)	−93
L-selectin ligand glycam-1 (14663)	−93
cadherin-8 (12564)	−95
purinergic receptor P2Y (18441)	−98
prothrombin (14061)	−102
GABA-A receptor alpha-1 (14394)	−102
norepinephrine transporter (20538)	−107
photolyase (12952)	−107
myelin-assoc. basic protein (17433)	−110
neuroendocrine convertase-2 (18549)	−112
ataxia telangiectasia/ATM (11920)	−115
5-HT receptor-2 (15558)	−117
granzyme B (14939)	−123
CRH receptor 2 (12922)	−123
estrogen-rel. receptor alpha (26379)	−126
antithrombin III (11905)	−132
secretogranin V (20394)	−148
prepro-orexin (15171)	−162
Day 7 After Aortic Perfusion	*Fold*
cdc25MM (19417)	−55
integrin alpha-2/CD49b (16398)	−56
LIM domain kinase-1 (16885)	−58
cytokeratin-18 (16668)	−59
antileukoproteinase-1 (20568)	−60
tubulin beta-4 (22153)	−62
AP endonuclease-1 (11792)	−65
Rab-3b (69908)	−65
SchC adaptor (20418)	−66
CAM kinase-GR (12326)	−68
collagen 9 alpha-1/COL9A1 (12839)	−69
prothrombin (14061)	−72
Day 7 After Aortic Perfusion	*Fold*
prothrombin (14061)	−72
bub1 mitotic checkpoint kinase (12235)	−74
tyrosine receptor kinase TRK-B (18212)	−74
plasminogen precursor (18815)	−76
c-Src-kinase and neg. regulator (12988)	−76
homeobox protein HOX-8 (17702)	−78
alpha-1 antitrypsin 1-2 (20701)	−79
interleukin-converting ICE (12362)	−81
ack tyrosine-protein kinase (51789)	−83
kinesin motor protein C2 (16581)	−83
zinc finger protein 144 (22658)	−89
semaphorin N (20359)	−91
proteasome component C8 (19167)	−98
GTPase-activating protein III (19414)	−107
homeobox protein D3 (15434)	−123
caspase-11 (12363)	−123
adenosine A3 receptor (11542)	−132
ACh receptor-assoc. RAPSYN (19400)	−132
Day 10 After Aortic Perfusion	*Fold*
transcription factor 3G (15377)	−60
chromobox homolog-4/CBX4 (12418)	−62
NIMA-rel. protein kinase 3 (23954)	−72
caudal type homeobox-2/Cdx2 (12591)	−76
zinc finger protein GLI3 (14634)	−91
homeobox protein D10 (15430)	−91
ephrin receptor A4 (13838)	−91
pou domain class 6F1 (19009)	−95
ephrin receptor A7 (13841)	−105
inhibin beta E (16326)	−105
semaphorin E (20348)	−107
G2/M-specific cyclin G2 (12452)	−110
filensin (12075)	−120
T cell activation linker ZAP-70 (16797)	−126
retinoic acid receptor gamma (20183)	−129
myosin light chain 1 atrial/fetal (17896)	−158
LIM homeobox protein 3 (16871)	−174
eyes absent homolog-1/EYA1 (14048)	−178
cadherin-15 (12555)	−195
TNF receptor-assoc.-4/TRAF4 (22032)	−209
Day 14 After Aortic Perfusion	*Fold*
mesenchyme homeobox-2 (17286)	−58
L-myc proto-oncogene (16918)	−98
cadherin-15 (12555)	−112
G2/mitotic-specific cyclin B1 (268697)	−115
homeobox protein D12 (15432)	−123
A-myb proto-oncogene (17864)	−141
galanin receptor 1 (14427)	−158
nociceptin (18155)	−162
N-myc proto-oncogene (18109)	−195
ephrin A3 (13638)	−204
G2/M-specific cyclin A2 (12428)	−204
GABA-A receptor alpha-1 (14394)	−219
5-HT receptor 1B (15551)	−257
neurogenin-3 (11925)	−269
cone-rod homeobox (12951)	−295

Analysis of the expression profiling dataset was used to identify significant differences in aortic wall gene expression at various intervals between the elastase perfusion groups compared to controls. The significance threshold for data analysis was set at $P < 0.01$ using the 2-tailed Z test, and genes were listed in rank-order based on the calculated relative fold-changes. Genes shown here include those with decreased expression of at least 50-fold in the elastase group compared to the heat-inactivated elastase control group (the complete list of genes with differential expression following elastase perfusion is shown in **Supplementary Data Table F,** on-line only).

elastase-induced AAAs are accompanied by temporally distinct patterns of increased expression for a variety of matrix-degrading proteinases, including MMPs, cathepsins, and serine proteinases; (3) at all time intervals of aneurysm development, there is a particularly marked increase in expression for genes encoding matricellular glycoproteins not previously associated with aneurysm disease, such as osteopontin, thrombospondin (TSP)-1,

and vitronectin; and (4) aneurysmal aortic tissues exhibit a decreased pattern of expression for genes encoding several different proteinase inhibitors, regulators of oxidative stress, and markers of smooth muscle cell function.

Recruitment and activation of inflammatory cells. Our findings confirm the suspicion that many genes induced during the early phases of elastase-induced aneurysm development are involved in inflammatory cell recruitment and activation. This included genes that encode acute phase reactants and leukocyte markers expressed at peak levels within 3 days of elastase perfusion, such as IL-6 (Fig 2, *A*), IL-1β (Fig 2, *B*), CD14/lipopolysaccharide receptor (Fig 2, *I*), integrin αL/CD11a, and integrin αM/CD11b (Fig 2, *M*). IL-6 is of particular interest because it is overexpressed in human AAA tissues and because circulating levels of IL-6 are increased in patients with AAAs.[19-22] This has led to the suggestion that IL-6 might act to induce the expression of extracellular matrix proteinases by mononuclear phagocytes and other cell types within aneurysm tissue, thereby serving as a proximal mediator of aneurysmal degeneration. Indeed, in recent studies we have found that elastase-induced aneurysms are associated with a substantial increase in IL-6 protein concentrations, both in aortic tissue and in the circulation, and that these levels are lower during pharmacologic suppression of AAAs.[16] These observations thereby provide strong evidence that the results obtained here for IL-6 expression are also reflected at the protein level in this model of AAAs.

Genes encoding several different chemokines were induced early after elastase perfusion (peak levels between day 3 and day 7), including MCP-3 (Fig 2, *C*), MIP-1α (Fig 2, *D*), MIP-1β (Fig 2, *E*), and MIP-2 (Fig 2, *F*). The proteins encoded by these genes are part of a structurally related family that exhibits chemotactic activity for mononuclear phagocytes.[23] Although the generation of high local concentrations of elastin degradation products is considered in large part responsible for stimulating the inflammatory cell response observed in elastase-induced AAAs, an early increase in medial smooth muscle cell expression of C-C chemokines (MCP-1 and regulated on activation, T cells expressed and secreted) indicates that these molecules may also play a role in establishing a chronic inflammatory response in the elastase-injured aorta.[24] This potential mechanism is further reinforced by the role of C-C chemokines in the formation of suprarenal aortic aneurysms in hypercholesterolemic mice.[25]

The expression patterns of MCP-3, MIP-1α, MIP-1β, and MIP-2 were all relatively similar but were different from the pattern exhibited by MIG, a C-X-C chemokine induced primarily at later stages of aneurysm formation (peak expression on day 14; Fig 2, *G*). Because MIG has prominent chemotactic activity for monocytes and because it was induced primarily during the late period of accelerated aortic dilatation, this chemokine may have a special role in sustaining and amplifying the chronic inflammatory response. The induction of MIG may also reflect a T-helper type 1 cellular immune response in elastase-induced AAAs, similar to that observed in the calcium chloride–induced mouse model of AAAs.[26] This may help to explain how elastase perfusion results in leukocyte recruitment into the outer aortic wall. It will therefore remain necessary to identify the cell types and mechanisms responsible for production of MIG and other chemokines within the elastase-injured aorta, as well as their functional importance in aneurysmal degeneration.

Matrix-degrading proteinases. Enzymatic degradation of structural extracellular matrix proteins is a key pathophysiologic process in aneurysmal degeneration. It is notable that among the matrix-degrading proteinases examined in this study, the expression of gelatinase A/MMP-2 was not significantly altered from the normal aorta or the control group at day 3 but progressively increased at later intervals when the increase in aortic diameter was most pronounced (Fig 3, *A*). Gelatinase B/MMP-9 exhibited a different pattern, with marked induction by day 3 and relatively diminished expression at later time intervals, but its expression was similar at all intervals between the elastase and control groups (Fig 3, *B*). A third pattern was observed for expression of MT1-MMP/MMP-14, which peaked on day 7 and increased again on day 14 but was also not significantly different at any interval between the elastase and control groups. Although each of these MMPs is also expressed in human aortic aneurysms, their temporally distinct patterns of expression in elastase-induced AAAs suggest that they may exert different roles in the stepwise progression of AAAs. Indeed, gene-targeting studies have revealed that MMP-9 (but not MMP-2) is required for development of elastase-induced AAAs,[12] whereas deficiency in either MMP-9 or MMP-2 results in suppression of calcium chloride–induced AAAs.[27]

We found that the early stages of aneurysm development were associated with a marked increase in the expression of dipeptidyl peptidase I (DPPI; cathepsin C), with a secondary increase at later phases of aneurysm expansion (Fig 3, *C*). The increase in DPPI was accompanied by a coincident decrease in expression of cystatin C, the principal endogenous inhibitor of cysteine proteases (Fig 3, *F*). This observation is of special interest given that DPPI can degrade extracellular matrix proteins and that circulating cystatin C levels are decreased in patients with both atherosclerosis and aortic aneurysms.[28,29] Further studies are therefore needed to elucidate the functional role of DPPI and other cysteine proteases in aneurysmal degeneration.

Matricellular glycoproteins. One of the important findings from this study is the marked increase in expression for several genes encoding matricellular glycoproteins, such as osteopontin and TSP-1. This finding suggests that they may help orchestrate tissue repair processes in the injured vascular wall. Thus, osteopontin increased more than 200-fold compared with normal aorta as early as 3 days after elastase perfusion (and 575-fold greater than the control group), and it remained substantially increased thereafter (Fig 3, *H*). Osteopontin is a multifunctional protein involved in the regulation of developmental osteogenesis,

wound repair, bacterial infection, and the innate immune response and has been shown to have a prominent role in cardiovascular injury and disease.[30,31] Osteopontin binds to interstitial and basement membrane collagens, as well as fibronectin,[32] and it acts as an adhesion substrate for cell migration through interactions with both αvβ3 integrin and the hyaluronan receptor CD44.[33,34] Osteopontin deficiency is associated with reduced collagen deposition and enhanced left ventricular dilatation after myocardial infarction, as well as attenuation of angiotensin-induced suprarenal aortic aneurysms, in hypercholesterolemic mice.[35,36] It will therefore be of great interest to test the hypothesis that osteopontin might also play a critical role in the elastase-induced mouse model of AAAs.

TSP-1 expression increased steadily during the development of aneurysmal degeneration, and maximal levels were reached by day 14 (Fig 3, *I*)—a significant pattern suggesting that this matricellular glycoprotein also participates in experimental AAA formation. TSP-1 potentially mediates a wide spectrum of complex functions in the vessel wall, where it is secreted by several different types of cells, including endothelium, vascular smooth muscle, and macrophages.[37-39] TSP-1 interacts with matrix proteins, as well as cell-surface receptors and adhesion molecules; moreover, it enhances smooth muscle cell proliferation and migration and platelet activation.[40,41] Additionally, TSP-1 is known to activate T lymphocytes, and its presence has been documented in human atheromatous lesions and experimental models of acute vascular injury and intimal hyperplasia.[42,43] A potential role for this protein in regulating the formation of aneurysms has yet to be explored.

Regulation of oxidative stress. Decreased expression in experimental AAAs may also yield clues as to the role of specific gene products in aneurysm formation. For example, glutathione-*S*-transferase 5 (Fig 3, *P*) belongs to a family of proteins that afford cellular protection against oxidative stress and toxins.[44] Oxidative stress can cause direct cellular injury, as well as the expression of vascular inflammatory gene products, and alterations in glutathione-*S*-transferases have been documented in human atherosclerotic disease.[45,46] The relative decrease in glutathione-*S*-transferase 5 messenger RNA observed throughout aneurysm development, therefore, indicates the potential relevance of oxidative stress in this murine model of AAAs. It is important to note that this observation is similar to the results obtained by Yajima et al,[18] thus supporting a general role for oxidative stress in aneurysm formation.

Limitations. The results of this study must clearly be taken in the context that despite many similarities, the pathophysiology of degenerative human AAAs may differ from the elastase-induced lesions observed in the laboratory. It is also important to reiterate that the development of elastase-induced AAAs is a dynamic process characterized by ongoing changes in aortic wall cellular composition, distribution, and number. Temporal changes in aortic wall gene expression therefore reflect the various cell types present, as well as the transcriptional activity for a given gene within a given cell population, and it remains to be determined whether the altered levels of expression for specific genes are due to changes in either resident aortic wall cell types (endothelium, medial smooth muscle, and fibroblasts), polymorphonuclear neutrophils recruited early and transiently in the response to the perfusion injury, or chronic inflammatory cells that appear later in the course of aneurysmal degeneration (monocyte-derived tissue macrophages, T cells, and B lymphocytes). Bone marrow–derived ($CD34^+$) circulating progenitor cells may also contribute to this process after mobilization and recruitment into the aortic wall.[47]

As in any expression profiling study, measures of relative tissue messenger RNA expression obtained with microarrays require further confirmation by other techniques before more functional studies are performed. Moreover, changes in messenger RNA are not always reflected by similar changes in protein production, and posttranslational modifications in protein are often just as crucial in regulating cellular behavior as are changes in gene transcription. Interpretation of large-scale cDNA expression data is further complicated by the large number of alterations typically observed for intracellular signaling proteins, transcription factors, and gene homologues with unknown function in mammalian systems.

Finally, it is difficult to anticipate which of the genes found to be differentially expressed in this study will be proven to be functionally significant in the process of aortic response to injury, inflammation, matrix remodeling, and aneurysmal degeneration. Knowledge of these temporal gene expression profiles will nonetheless be helpful in guiding further studies on the molecular mechanisms underlying aneurysmal degeneration and will be especially valuable for investigations involving mice with specific genetic alterations.

REFERENCES

1. Tung WS, Lee JK, Thompson RW. Simultaneous analysis of 1176 gene products in normal human aorta and abdominal aortic aneurysms using a membrane-based complementary DNA expression array. J Vasc Surg 2001;34:143-50.
2. Armstrong PJ, Johanning JM, Calton WC Jr, Delatore JR, Franklin DP, Han DC, et al. Differential gene expression in human abdominal aorta: aneurysmal versus occlusive disease. J Vasc Surg 2002;35:346-55.
3. Absi TS, Sundt TM III, Tung WS, Moon M, Lee JK, Damiano RR Jr, et al. Altered patterns of gene expression distinguishing ascending aortic aneurysms from abdominal aortic aneurysms: complementary DNA expression profiling in the molecular characterization of aortic disease. J Thorac Cardiovasc Surg 2003;126:344-57.
4. Dobrin PB. Animal models of aneurysms. Ann Vasc Surg 1999;13: 641-8.
5. Thompson RW, Geraghty PJ, Lee JK. Abdominal aortic aneurysms: basic mechanisms and clinical implications. Curr Probl Surg 2002;39: 110-230.
6. Anidjar S, Salzmann JL, Gentric D, Lagneau P, Camilleri JP, Michel JB. Elastase-induced experimental aneurysms in rats. Circulation 1990;82: 973-81.
7. Halpern VJ, Nackman GB, Gandhi RH, Irizarry E, Scholes JV, Ramey WG, et al. The elastase infusion model of experimental aortic aneurysms: synchrony of induction of endogenous proteinases with matrix destruction and inflammatory cell response. J Vasc Surg 1994;20:51-60.
8. Ricci MA, Strindberg G, Slaiby JM, Guibord RS, Bergersen LJ, Nichols PP, et al. Anti-CD18 monoclonal antibody slows experimental aortic aneurysm expansion. J Vasc Surg 1996;23:301-7.

9. Holmes DR, Petrinec D, Wester W, Thompson RW, Reilly JM. Indomethacin prevents elastase-induced abdominal aortic aneurysms in the rat. J Surg Res 1996;63:305-9.
10. Petrinec D, Liao S, Holmes DR, Reilly JM, Parks WC, Thompson RW. Doxycycline inhibition of aneurysmal degeneration in an elastase-induced rat model of abdominal aortic aneurysm: preservation of aortic elastin associated with suppressed production of 92 kD gelatinase. J Vasc Surg 1996;23:336-46.
11. Bigatel DA, Elmore JR, Carey DJ, Cizmeci-Smith G, Franklin DP, Youkey JR. The matrix metalloproteinase inhibitor BB-94 limits expansion of experimental abdominal aortic aneurysms. J Vasc Surg 1999;29: 130-8.
12. Pyo R, Lee JK, Shipley JM, Curci JA, Mao D, Ziporin SJ, et al. Targeted gene disruption of matrix metalloproteinase-9 (gelatinase B) suppresses development of experimental abdominal aortic aneurysms. J Clin Invest 2000;105:1641-9.
13. Lee JK, Borhani M, Ennis TL, Upchurch GRJ, Thompson RW. Experimental abdominal aortic aneurysms in mice lacking expression of inducible nitric oxide synthase. Arterioscler Thromb Vasc Biol 2001; 21:1393-401.
14. Eliason JL, Hannawa KK, Ailawadi G, Sinha I, Ford JW, Deogracias MP, et al. Neutrophil depletion inhibits experimental abdominal aortic aneurysm formation. Circulation 2005;112:232-40.
15. Hannawa KK, Eliason JL, Woodrum DT, Pearce CG, Roelofs KJ, Grigoryants V, et al. L-selectin-mediated neutrophil recruitment in experimental rodent aneurysm formation. Circulation 2005;112:241-7.
16. Parodi FE, Mao D, Ennis TL, Bartoli MA, Thompson RW. Suppression of experimental abdominal aortic aneurysms in mice by treatment with pyrrolidine dithiocarbamate, an antioxidant inhibitor of nuclear factor-kappaB. J Vasc Surg 2005;41:479-89.
17. Cheadle C, Vawter MP, Freed WJ, Becker KG. Analysis of microarray data using Z score transformation. J Mol Diagn 2003;5:73-81.
18. Yajima N, Masuda M, Miyazaki M, Nakajima N, Chien S, Shyy JY. Oxidative stress is involved in the development of experimental abdominal aortic aneurysm: a study of the transcription profile with complementary DNA microarray. J Vasc Surg 2002;36:379-85.
19. Szekanecz Z, Shah MR, Pearce WH, Koch AE. Human atherosclerotic abdominal aortic aneurysms produce interleukin (IL)-6 and interferon-gamma but not IL-2 and IL-4: the possible role for IL-6 and interferon-gamma in vascular inflammation. Agents Actions 1994;42:159-62.
20. Juvonen J, Surcel HM, Satta J, Teppo AM, Bloigu A, Syrjala H, et al. Elevated circulating levels of inflammatory cytokines in patients with abdominal aortic aneurysm. Arterioscler Thromb Vasc Biol 1997;17: 2843-7.
21. Rohde LE, Arroyo LH, Rifai N, Creager MA, Libby P, Ridker PM, et al. Plasma concentrations of interleukin-6 and abdominal aortic diameter among subjects without aortic dilatation. Arterioscler Thromb Vasc Biol 1999;19:1695-9.
22. Jones KG, Brull DJ, Brown LC, Sian M, Greenhalgh RM, Humphries SE, et al. Interleukin-6 (IL-6) and the prognosis of abdominal aortic aneurysms. Circulation 2001;103:2260-5.
23. Rossi D, Zlotnik A. The biology of chemokines and their receptors. Annu Rev Immunol 2000;18:217-42.
24. Colonnello JS, Hance KA, Shames ML, Wyble CW, Ziporin SJ, Leidenfrost JE, et al. Transient exposure to elastase induces mouse aortic wall smooth muscle cell production of MCP-1 and RANTES during development of experimental aortic aneurysm. J Vasc Surg 2003;38: 138-46.
25. Ishibashi M, Egashira K, Zhao Q, Hiasa K, Ohtani K, Ihara Y, et al. Bone marrow-derived monocyte chemoattractant protein-1 receptor CCR2 is critical in angiotensin II-induced acceleration of atherosclerosis and aneurysm formation in hypercholesterolemic mice. Arterioscler Thromb Vasc Biol 2004;24:e174-8.
26. Xiong W, Zhao Y, Prall A, Greiner TC, Baxter BT. Key roles of CD4(+) T cells and IFN-gamma in the development of abdominal aortic aneurysms in a murine model. J Immunol 2004;172:2607-12.
27. Longo GM, Xiong W, Greiner TC, Zhao Y, Fiotti N, Baxter BT. Matrix metalloproteinases 2 and 9 work in concert to produce aortic aneurysms. J Clin Invest 2002;110:625-32.
28. Wolters PJ, Laig-Webster M, Caughey GH. Dipeptidyl peptidase I cleaves matrix-associated proteins and is expressed mainly by mast cells in normal dog airways. Am J Respir Cell Mol Biol 2000;22:183-90.
29. Shi GP, Sukhova GK, Grubb A, Ducharme A, Rhode LH, Lee RT, et al. Cystatin C deficiency in human atherosclerosis and aortic aneurysms. J Clin Invest 1999;104:1191-7.
30. Giachelli CM, Liaw L, Murry CE, Schwartz SM, Almeida M. Osteopontin expression in cardiovascular diseases. Ann N Y Acad Sci 1995;760:109-26.
31. Denhardt DT, Noda M, O'Regan AW, Pavlin D, Berman JS. Osteopontin as a means to cope with environmental insults: regulation of inflammation, tissue remodeling, and cell survival. J Clin Invest 2001; 107:1055-61.
32. Mukherjee BB, Nemir M, Beninati S, Cordella-Miele E, Singh K, Chackalaparampil I, et al. Interaction of osteopontin with fibronectin and other extracellular matrix molecules. Ann N Y Acad Sci 1995;760: 201-12.
33. Denhardt DT, Lopez CA, Rollo EE, Hwang SM, An XR, Walther SE. Osteopontin-induced modifications of cellular functions. Ann N Y Acad Sci 1995;760:127-42.
34. Weber GF, Ashkar S, Glimcher MJ, Cantor H. Receptor-ligand interaction between CD44 and osteopontin (Eta-1). Science 1996;271: 509-12.
35. Trueblood NA, Xie Z, Communal C, Sam F, Ngoy S, Liaw L, et al. Exaggerated left ventricular dilation and reduced collagen deposition after myocardial infarction in mice lacking osteopontin. Circ Res 2001; 88:1080-7.
36. Bruemmer D, Collins AR, Noh G, Wang W, Territo M, Arias-Magallona S, et al. Angiotensin II-accelerated atherosclerosis and aneurysm formation is attenuated in osteopontin-deficient mice. J Clin Invest 2003;112:1318-31.
37. Reed MJ, Iruela-Arisp L, O'Brien ER, Truong T, LaBell T, Bornstein P, et al. Expression of thrombospondins by endothelial cells: injury is correlated with TSP-1. Am J Pathol 1995;147:1068-80.
38. Mumby SM, Abbott Brown D, Raugi D, Bornstein P. Regulation of thrombospondin secretion by cells in culture. J Cell Physiol 1984;120: 280-8.
39. Jaffe EA, Ruggiero JT, Falcone DJ. Monocytes and macrophages synthesize and secrete thrombospondin. Blood 1985;65:79-84.
40. Majack RA, Cook SC, Bornstein P. Control of smooth muscle cell growth by components of the extracellular matrix: autocrine role for thrombospondin. Proc Natl Acad Sci U S A 1986;83:9050-4.
41. Nesselroth SM, Willis AI, Fuse S, Olson ET, Lawler J, Sumpio BE, et al. The C-terminal domain of thrombospondin-1 induces vascular smooth muscle cell chemotaxis. J Vasc Surg 2001;33:595-600.
42. Vallejo AN, Mugge LO, Klimiuk PA, Weyand CM, Goronzy JJ. Central role of thrombospondin-1 in the activation and clonal expansion of inflammatory T cells. J Immunol 2000;164:2947-54.
43. Chen D, Ashara T, Krasinski K, Witzenbichler B, Yang J, Magner M, et al. Antibody blockade of thrombospondin accelerates reendothelialization and reduces neointima formation in balloon-injured rat carotid artery. Circulation 1999;100:849-54.
44. Hayes JD, Strange RC. Glutathione-S-transferase polymorphisms and their biological consequences. Pharmacology 2000;61:154-66.
45. Kunsch C, Medford RM. Oxidative stress as a regulator of gene expression in the vasculature. Circ Res 1999;85:753-66.
46. Izzotti A, Cartiglia C, Lewtas J, De Flora S. Increased DNA alterations in atherosclerotic lesions of individuals lacking the GSTM1 genotype. FASEB J 2001;15:752-7.
47. Sho E, Sho M, Nanjo H, Kawamura K, Masuda H, Dalman RL. Hemodynamic regulation of CD34+ cell localization and differentiation in experimental aneurysms. Arterioscler Thromb Vasc Biol 2004; 24:1916-21.

Submitted Sep 6, 2005; accepted Jan 6, 2006.